Colloid Polym Sci (2007) 285:1313–1319
DOI 10.1007/s00396-007-1688-7

Synthesis and electrical, rheological and thermal characterization of conductive polyurethane

Syang-Peng Rwei · Leeyih Wang

Received: 27 February 2007 / Accepted: 27 April 2007 / Published online: 31 May 2007

Abstract This work studies the electrical, rheological, and thermal characteristics for polyurethane (PU) capped with tetraaniline as a new material, tetraaniline-containing poly (urethane–urea) (TAPU). The conductivities can be increased from less than 10^{-10} S/cm for pure PU to 10^{-4} S/cm for TAPU, independently of the length of the soft segment in the TAPU backbone chain. The tensile strength and modulus are increased when PU is copolymerized with tetraaniline. The viscoelastic creep can be effectively simulated using a Burgers model. Additionally, TAPU has higher viscosity, higher retardation time, and lower compliance J_1 than regular PU. Restated, TAPU exhibits less elastic but superior permanent deformation than PU because tetraaniline functions as a chain holder. The thermogravimetric analytic (TGA) results reveal that TAPU has lower T_d, smaller T_{mw1} and T_{mw2}, and higher char yield because the dehydration of the urea-containing polymer produces a thin layer from a nitrogen compound on the polymer's surface, which insulates the underlying polymer from heat and oxygen.

Keywords Tetraaniline-containing poly (urethane–urea) (TAPU) · Conductivity · Viscoelastic creep · Compliance · Thermal degradation

S.-P. Rwei (✉)
Institute of Organic and Polymeric Materials,
National Taipei University of Technology,
#1, Sec. 3, Chung-Hsiao E. Rd.,
Taipei, Taiwan
e-mail: f10714@ntut.edu.tw

L. Wang
Center of Condensed Matter Science, National Taiwan University,
Taipei, Taiwan

Introduction

Polyurethane (PU), developed in the early 1940s, exhibits such favorable properties as high elasticity, high abrasion resistance, excellent resistance to gas, and high reactivity in the reaction injection molding process. Given its many favorable properties, and especially super elasticity, most PU is used in elastomer applications [1–5]. However, conductive polymers with conjugated chains are commonly classified as rigid, brittle, and difficult to process but they exhibit unique electric conductivity [6–11]. Accordingly, much research effort has been made to overcome the deficiencies of conductive polymers. One common method is to incorporate thermal plastics or flexible macromolecules such as PU into conjugated polymer to make polymer composites. The disadvantage of this procedure arises from the expected low compatibility of rigid conjugated chains with the hosting elastomers, which results in the severe phase separation and the loss of matrix elasticity and material conductivity. In this work, oligoaniline chains were chemically added to both chain-ends of the urethane prepolymer to form elastomeric conductive copolymer. An elastomer with favorable physical conductivity, elasticity, and thermal endurance is expected to be generated thereafter.

Experimental

Material preparation Poly(tetramethylene glycol) (PTMO) obtained from ACROS was dehydrated at 80 °C in vacuum for 8 h before use. Triethylamine (Aldrich) and tetrahydrofuran (THF; Mallinckrodt) were dried and distilled over CaH_2 and Na, respectively. *N*,*N*′-dimethylformamide (DMF; Pharmco) was purified by passing through a BaO column, and then distilled at reduced pressure and subse-

quently over four A molecular sieves. 4,4′-Diphenylmethane diisocyanate (MDI; TCI) was melted at 50 °C, and only the liquid portion was used. The tetraaniline was synthesized by adding dianiline into 0.1 M HCl, catalyzing with iron (III) chloride at room temperature following the method proposed by MacDiarmid et al. [11]. The tetraaniline was then doped with dodecylbenzenesulfonic acid (DBSA) [12–16] to ensure good conductivity and compatibility with PU.

Synthesis of tetraaniline-containing poly(urethane–urea), ***1*** A flask equipped with a mechanical stirrer and an inert gas bubbler was charged with dehydrated PTMO and MDI in a mole ratio of 1:2. The mixture was stirred at 65 °C under N_2 for 4 h to yield the prepolymer ***2***, diisocyanate-capped urethane. Notably, the prepolymer ***2*** was prepared freshly because of the sensitivity of isocyanate groups to moisture. Preopolymer ***2*** was dissolved in a solution of mixed DMF/THF (v/v=1), and then tetraaniline solution [tetraaniline (11 g)/DMF (100 ml)] and 2 ml of the catalyst, triethylamine, were added in that order. The solution was then maintained for 4 h at 60 °C under N_2. The mole ratio of prepolymer ***2*** to tetraaniline was 1:3. The solution was then poured into cold ether to cause precipitation and was purified with ether to remove excess tetraaniline and linear cooligomer.

Characterization Gel permeation chromatography (GPC) was performed on a Jasco PU-1580 GPC at 40 °C with three linear Jordi columns. THF was adopted as the carrier solvent at a flow rate of 1.0 ml/min. Infrared and UV-vis spectra were obtained using a Jasco FT/IR-480 and Hitachi U- 3410 spectraphotometer, respectively. Thermogravimetric analytic (TGA) thermograms were obtained using a Perkin–Elmer TGA-7 in a dry nitrogen atmosphere at the set heating rate. The mechanical characteristics were measured using a Perkin–Elmer DMA-7e in a tensile mold or creep mode. The electric conductivity was measured using a 236 source measure unit (Keithley) on a cell with four detecting points.

Results and discussion

The Fourier transform infrared (FTIR) spectrum of tetraaniline-containing poly(urethane–urea) (TAPU) 2000, unlike that of PU [17] (all in Fig. 1), exhibited intense adsorption centered at 1,510 cm^{-1}, corresponding to benzoid C=C stretching in the tetraaniline unit. Additionally, the presence of adsorption peaks centered at 1,721 and 1,661 cm^{-1}, corresponding to NH and NCO in a urea group (–NH–CO–NH–), reveals the formation of a urea linkage inside TAPU 2000, respectively.

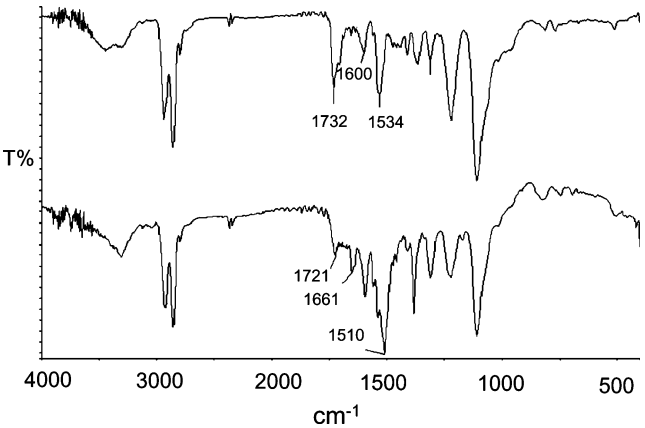

Fig. 1 The FTIR spectrum of TAPU

GPC studies revealed that the average numerical molecular weights (M_n) of prepolymer ***2*** 2000, copolymer ***1*** TAPU 2000, and PU 2000 were 6,190, 7,520 (Fig. 2), and 42,930 g/mole, respectively, based on the calibration curve established by polystyrene standards. The polydispersity of copolymer ***1*** (2.24) was found to be very close to that of prepolymer ***2*** 2000 (2.15). This observation demonstrates that the urea coupling reactions did not broaden the mass distribution of the parent polyether. Table 1 presents all of the GPC results obtained under various PU and TAPU conditions. The data show that the M_n of PU is three to five times that of TAPU because the tetraaniline functions as a terminator in further condensation polymerization. In fact, the lower M_n of TAPU supports a conductive PU with satisfactory elasticity and conductivity. A detailed discussion will be presented later.

Table 2 presents T_g values of PU and TAPU obtained using DMA. The T_g values decreased as the PTMO length

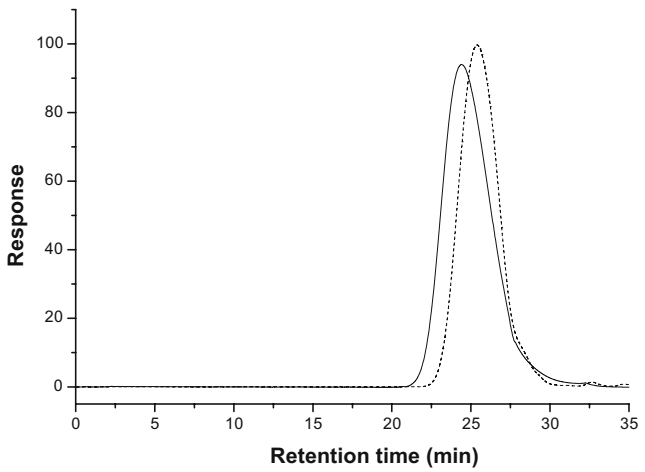

Fig. 2 The average number molecular weights (M_n) of prepolymer ***2*** 2000, copolymer ***1*** TAPU 2000, and PU 2000 as revealed by GPC studies

Table 1 The GPC results of the molecular weight for various PU and TAPU

	M_n	M_w	PDI
TAPU 1000	5,180	10,670	2.06
TAPU 1400	6,120	12,350	2.02
TAPU 2000	7,520	16,850	2.24
TAPU 2900	6,840	15,110	2.21
PU 1000	13,180	30,610	2.32
PU 1400	20,170	39,050	2.00
PU 2000	42,930	93,520	2.18
PU 2900	20,590	43,250	2.10

increased because the flexibility of polymer main chains increases with the length of PTMO. Additionally, the difference between the T_g of PU capped with tetraaniline and that with no cap was 15°. Incorporating tetraaniline, a bulky rigid aromatic group increases the rotational barrier of the PU chain. The barrier may suppress molecular mobility and, thereby, increase T_g.

Figure 3 plots the stress–strain curve for PU copolymers with soft segments of various lengths and capped or not capped tetraaniline. The tensile strength and modulus increased when PU is copolymerized with tetraaniline. The tensile strength and modulus increase by a factor of two to eight and four to eight, respectively, as the lengths of the PU soft segments that participate in the reaction increase. This interesting finding may be attributed to tetraaniline acting as a hard segment that holds the PU chains, and then forms a sturdy network. The elongation declines by roughly 20%, the value that is reasonable and tolerable for a material with enhanced crosslinking and used in an engineering application. The molecular weight (M_n) of PU 2000 is three times that of TAPU. However, that the latter exhibits only a 20% drop in elongation is quite surprising. Briefly, capping PU with tetraaniline improves the mechanical properties without significantly degrading elongation performance.

Table 2 presents the experimental results of conductivity for both PU and TAPU. The conductivities of pure PU materials were all less than 10^{-10} S/cm, indicating a total absence of conductivity. In contrast, experimental data

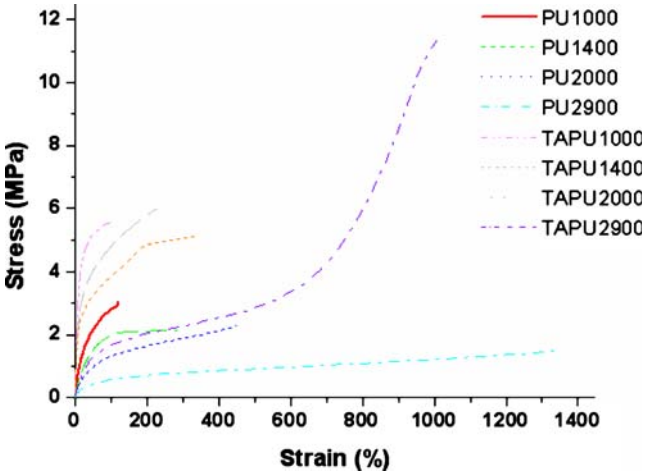

Fig. 3 The stress–strain curve for PU copolymers with soft segments of various lengths and capped or not capped tetraaniline

reveal that the conductivity can increase by six orders of magnitude when tetraaniline was capped with PU. Table 2 demonstrates that an increase in the length of the soft segment from PTMO 650 to PTMO 2000 only very slightly affects the conductivity. However, elongation improves greatly, as mentioned above. Additionally, the TAPU 2900, which has much greater elongation and tensile strength, maintains a conductivity of 4.3×10^{-4} S/cm and is, thus, a superior elastomeric material with favorable antistatic properties. Notably, the conductivity presented herein is much better than the way of direct blending PU with tetraaniline or with PU-tetraaniline copolymer (tetraaniline rich) whose conductivities are around 10^{-8} S/cm [16].

Figure 4 presents typical creep behaviors [18] of PU and TAPU elastomers. The solid line represents experimental data that are fitted closely by a Burgers model [19], as demonstrated by the dashed-dotted line. A constant elongation strength, approximately 0.007 MPa (200 mNT/30 mm^2), was applied in the creep test. Notably, the applied strength is far below the yielding point of the stress–strain curve for each sample (Fig. 3) to ensure the test was conducted in a linear-viscoelastic range. Table 3 lists all of the fitting parameters in the Burgers model under various PU and TAPU conditions. The Burgers model is a four-

Table 2 The T_g, conductivity, and degradation E_a for various PU and TAPU

	PU 1000	TAPU 1000	PU 1400	TAPU 1400	PU 2000	TAPU 2000	PU 2900	TAPU 2900
T_g (°C)	−48.5	−34.9	−55.1	−42.7	−59.9	−45.1	−64.7	−59.7
Conductivity (S/cm)	$<10^{-10}$	3.1×10^{-4}	$<10^{-10}$	3.63×10^{-4}	$<10^{-10}$	8.4×10^{-4}	$<10^{-10}$	4.1×10^{-6}
E_a (average), mean E_a of degradation; KJ/mol)	139.7	145.7	152.2	168.7	161.7	187.7	171.7	193.2

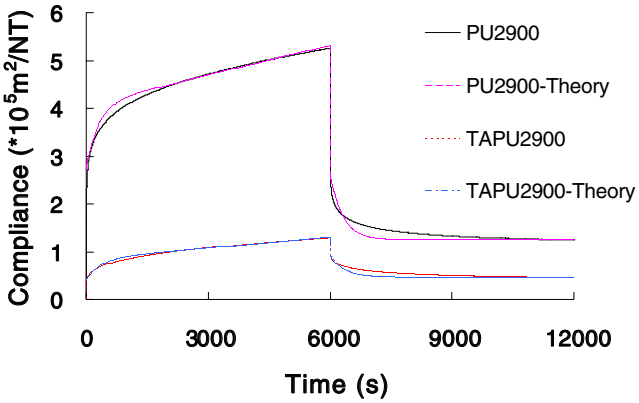

Fig. 4 Typical creep behaviors of PU and TAPU elastomers

parameter viscoelastic model that consists of a Kelvin and Maxwell model in series. The data following this mechanical analog demonstrate an initial elastic response due to the free spring, the retarded elastic behavior associated with the parallel spring–dashpot combination and Newtonian flow after long periods caused by the free dashpot. The Burgers model can also be expressed in terms of creep compliance:

$$J_c(t_1) = J_0 + J_1(1 - \exp(-t_1/T_S)) + t_1/\eta_0 \quad (1)$$

$$J_r(t_1) = J_c(t_1) - \{J_1(1 - \exp(-(t - t_1)/T_S)) + J_0^*\} \quad (2)$$

In general, a linear viscoelastic material would exhibit a nonlinear response to strain due to their incapability to completely recover the structure by storing energy in the elastic part. A permanent deformation owing to the viscous loss was, therefore, observed [20]. The strain recovery, or creep recovery, is also called recoil and may be studied with reference to a recoil function.

The driving force for creep recovery of PU material typically has two resources. First, entropy increases when an individual chain between junction points recoils from an extended state to a relaxed state. Secondly, the entropy increases when the whole PU chain adopts a new shape. The end-to-end distance of the PU chain, independently of the light strain associated with a few junction points inside the chain, decreases in the stress direction to a small length in the relaxed state.

The instantaneous creep response and creep recovery, J_0 and J_0^*, are determined mainly by the rubbery elasticity of the PU network. The well-known Phantom model can describe the physical behaviors of the network. The junction points of the phantom network can fluctuate about the mean values, and the chains between the crosslinks can take any of the very many possible conformations. Ideally, J_0^* equals J_0 based on the Phantom model. However, in Table 3, J_0^* is approximately 10 to 20% lower than J_0; dislocation or even disconnection of the junction points may occur during the creep test, reducing the elasticity. Table 3 presents another interesting result: J_0 and J_0^* of TAPU are five to six times smaller than those of PU. Clearly, tetraaniline functions not only as a chain-end cap but also as a junction point. The chain length between junction points, therefore, decreases as do J_0 or J_0^*. This result is consistent with the tensile result, confirming that PU was hardened when tetraaniline was incorporated [21].

The time-dependent creep responses can be well described by a combination of the free dashpot and Kelvin model, denoted as t_1/η_0 and $J_1(1-\exp(-t_1/\tau_s))$, respectively. The free dashpot represents a permanent deformation in the material related to t_1/η_0. Some local regions that are free of junction points do exist in the lightly crosslinked PU. When the stress exceeds a yield value, the chains in the local region deform first, and then flow in the stress direction because of an absence of holding points. Once the stress has been removed, the end-to-end distance in the stress direction of the PU chain decreases from a large value in a stretched state to a small value in the relaxation state. The constraint on the chain by the increase in entropy can be described by the Kelvin model in recovery mode. However, the permanent deformation caused by the flow is irreversible and can be represented by a

Table 3 The fitting results of the Burgers model for various PU and TAPU

	J_0 (m^2/NT)	J_1 (m^2/NT)	J_0^* (m^2/NT)	τ_s (s)	η_0 (Pa s)
PU 1000	5.51×10^{-6}	1.76×10^{-6}	4.62×10^{-6}	485	5.19×10^{9}
PU 1400	7.38×10^{-6}	3.82×10^{-6}	6.21×10^{-6}	430	3.16×10^{9}
PU 2000	13.02×10^{-6}	3.01×10^{-6}	11.52×10^{-6}	370	2.51×10^{9}
PU 2900	26.77×10^{-6}	13.87×10^{-6}	25.7×10^{-6}	300	0.48×10^{9}
TAPU 1400	1.46×10^{-6}	0.82×10^{-6}	1.11×10^{-6}	626	11.15×10^{9}
TAPU 2000	1.95×10^{-6}	3.62×10^{-6}	2.72×10^{-6}	510	5.54×10^{9}
TAPU 2900	3.91×10^{-6}	4.43×10^{-6}	3.79×10^{-6}	344	1.31×10^{9}

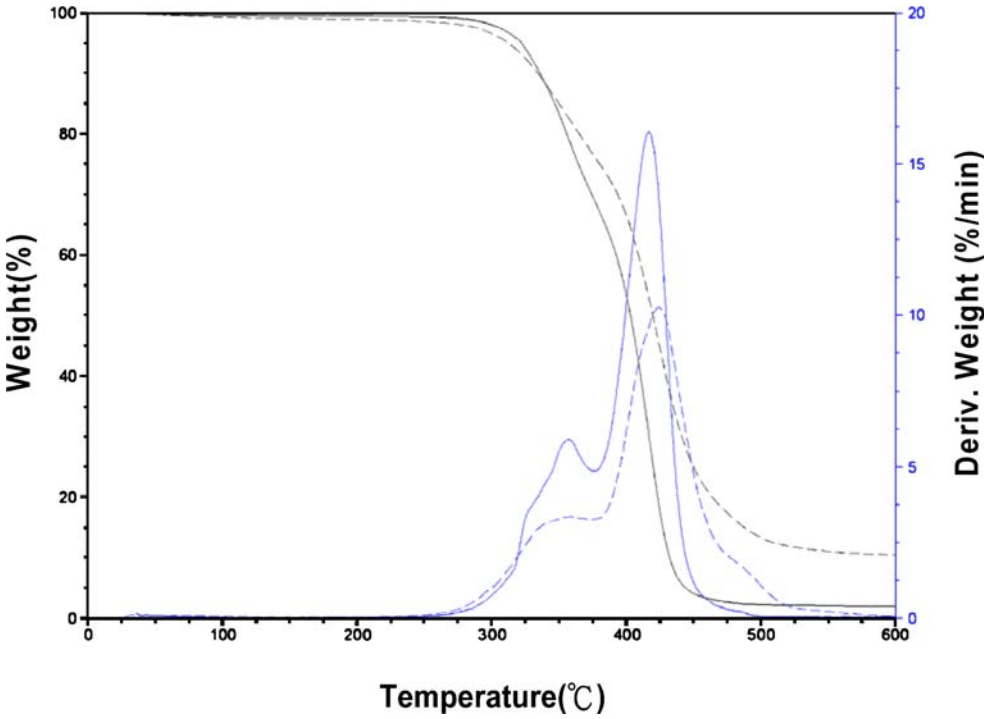

Fig. 5 Typical TGA thermograms of TAPU 2000 and PU 2000 at the heating rate of 10 °C/min in nitrogen

free dashpot model. Table 3 reveals that TAPU has a higher viscosity, higher retardation time, and lower compliance J_1 than regular PU. TAPU with a longer retardation time and a higher viscosity indicates that the time to reach its full deformation is slower. Also, the permanent deformation is small because tetraaniline functions as a chain retarder [22]. Briefly, TAPU exhibits lower elastic but better permanent deformation than PU because tetraaniline serves as a chain holder.

Thermogravimetric analysis (TGA) is the conventional technique for evaluating the thermal stability of polymers. Figure 5 presents typical TGA thermograms of TAPU 2000 and PU 2000 at the heating rate of 10 °C/min in nitrogen. The rate of degradation at a specific temperature is given by the tangential slope of a TGA trace. The temperature of initial degradation, T_d, the rates of weight loss T_{mw1} and T_{mw2}, and the residual weight fraction, called the char yield, are typically of primary importance. Table 4 compares TGA analyses of various PU and TAPU at a heating rate of 10 °C/min. The table demonstrates that TAPU has lower T_d, slower T_{mw1} and T_{mw2}, and higher char yield. The relatively low initial stability T_d of TAPU is explained by the electrophilic characteristics of the carbonyl group because the ionized urea group facilitates the transfer of hydrogen from the positively to the negatively charged nitrogen followed by bond dissociation. Accordingly, the TAPU samples have lower initial degradation temperature T_d.

The TGA curves of both PU and TAPU have two distinct regions of weight loss, indicating two stages of thermal degradation [23–28]. A review on PU degradation reveals that thermal stability and degradation depend on the type of the hard and soft segments in the backbone of the

Table 4 TGA analysis of various PU and TAPU

	T_d (°C)	T_{mw1} (%/min)	T_{mw2} (%/min)	Char yield (%)
PU 1000	306.3	8.6	9.7	3.4
TAPU 1000	301.7	4.6	8.5	12.7
PU 1400	308.4	6.8	14.8	3.3
TAPU 1400	301.3	3.5	9.6	11.9
PU 2000	320.2	5.8	16.2	2.1
TAPU 2000	312.5	3.2	10.2	14.5
PU 2900	319.5	4.2	16.2	3.7
TAPU 2900	313.9	2.9	12.1	10.5

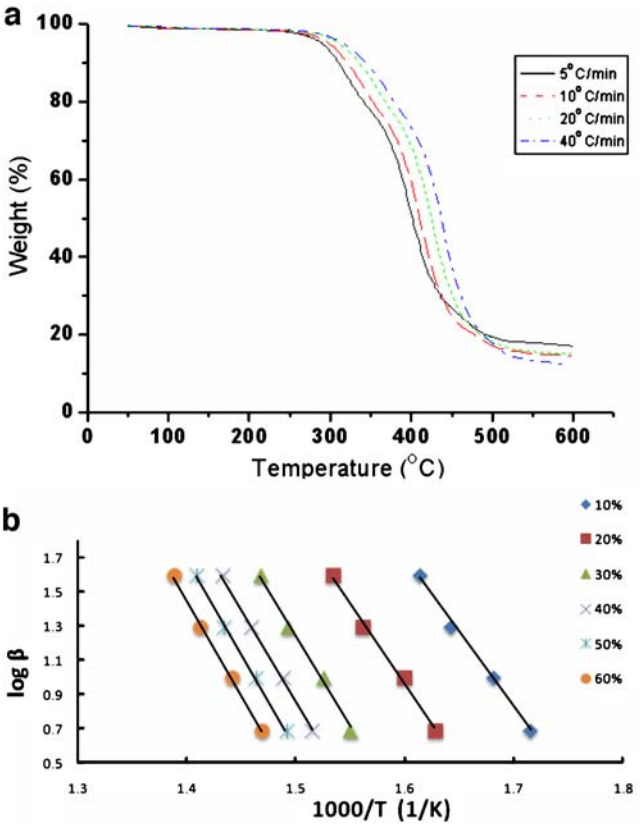

Fig. 6 **a** The activation energy (E_a) of degradation for a given TGA weight fraction. **b** TGA curves at various heating rates (β)

polymers. The initial step of the degradation in stage I involves primarily the decomposition of the hard segment by the dissociation of urethane or urea to the original polyol and isocyanate, forming a primary amine, alkene, and carbon dioxide. However, stage II proceeds by depolycondensation and polyol degradation mechanisms, and is influenced by the soft segment content. Experimental results demonstrated that a sample in which PTMG 2000 is the soft segment was more thermally stable in stage I, while a sample in which PTMG 1000 is the soft segment was more thermally stable in stage II. Additionally, the PU degradation mechanisms described above can be applied to explain clearly why the weight loss rates in stages I and II, T_{mw1} and T_{mw2} in Table 4, decrease and increase, respectively, as the length of PTMG increases. Table 4 expresses another interesting result: The rate of weight loss during degradation can be reduced by capping PU with tetraaniline. After the initial degradation in stage I, the libration of amine by the decomposition of the urea segment has been reported to stabilize the polyether segment, promoting thermal stability. In the early stage of decomposition, the dehydration of the urea-containing polymer is initiated, yielding a thin layer of a nitrogen compound on the polymer's surface, insulating the underlying polymer from heat and oxygen. Therefore, TAPU has a lower loss-rate for both T_{mw1} and T_{mw2}, and a significantly higher char yield than PU, indicating less degradation in stages I and II (Table 4).

The activation energy (E_a) of degradation for a given TGA weight fraction (weight percent) can be obtained by Ozawa's method (Eq. 3) [29–31]. This approach depends on several TGA curves at various heating rates (β). Accordingly, a plot of $\log(\beta)$ against T^{-1} should be a straight line with a slope of $0.457E_a/R$ (Fig. 6a,b). The mean activation energy could be calculated by averaging out the E_a values obtained from Eq. 3 for each conversion ratio. The mean E_a values of the PU and TAPU series were determined and the results summarized in Table 2. The TAPU had higher E_a values at all PTMO lengths, reconfirming that capping PU with tetraaniline, as described above, improves thermal stability.

$$E_a = 2.19 * R * d[\log(\beta)]/d[1/T] \quad (3)$$

Conclusions

This work investigates the electrical, rheological, and thermal properties for PU capped with tetraaniline to form a new material, tetraaniline-containing poly(urethane–urea) (TAPU). The results yield the following conclusions:

1. The conductivities can be improved from 10^{-10} S/cm for pure PU to 10^{-4} S/cm for TAPU, independently of the length of soft segment within TAPU backbone chain.
2. The tensile strength and modulus are increased when PU is copolymerized with tetraaniline.
3. The viscoelastic creep for both PU and TAPU can be effectively simulated using a Burgers model. TAPU has higher viscosity, higher retardation time, and lower compliance J_1 than regular PU because tetraaniline functions as a chain holder.
4. The TGA results reveal that TAPU has lower T_d, smaller T_{mw1} and T_{mw2}, and higher char yield because the dehydration of the urea-containing polymer produces a thin layer from a nitrogen compound on the polymer's surface, which insulates the underlying polymer from heat and oxygen.

Acknowledgment The authors would like to thank the National Science Council of the Republic of China, Taiwan, for financially supporting this research under contract no. NSC 94-2622-E-027-003-CC3.

References

1. Onder K, Peters RH, Spark LC (1977) Polymer 8:155–160
2. Spathis G, Niaounakis M, Kontou E, Apekis L, Pissis P, Christwodoulides C (1994) J Appl Polym Sci 54:831–842
3. Aimin C, Shishan W, Dingjun J, Fen W, Jian S (2005) Colloid Polym Sci 283:880
4. Kontou E, Spathis G, Niaounakis M, Kefalas V (1990) Colloid Polym Sci 268:636
5. Godovsky YK, Bessonova NP (1983) Colloid Polym Sci 261:645
6. Meyer WH (1998) Adv Mater 10:439–448
7. Trivedi DC (1997) In: Nalwa HS (ed) Handbook of organic conductive molecules and polymers, vol. 2. Wiley, New York, p 548
8. Fong YF, Svhlenoff JB (1995) Polymers 36:639–649
9. MacDiarmid AG, Heeger AJ (1979) Synth Met 1:101–118
10. Wessling B (1991) Synth Met 1:119–149
11. MacDiarmid AG, Epstein AJ, Zhang WJ, Feng J (1997) Synth Met 84:119–120
12. Nigrey PJ, Macinnes DF (1981) J Electrochem Soc 128:1651–1654
13. Allen WN, Prant P, Carosella CA (1978) Synth Met 1:151–159
14. Tlarke TC, Krounbi MT, Lee VY (1981) J Chem Soc:384
15. MacDiarmid AG, Epstein AJ (1994) Synth Met 65:103–116
16. Wang YZ, Hsu YC, Chou LC, Hsieh KH (2004) J Polym Res 11:127–132
17. Coleman MM, Skrovanek DJ, Hu J, Painter PC (1988) Macromolecules 21:59–65
18. Plashchina G, Grinberg NV, Braudo EE, Tolstoguzov VB (1980) Colloid Polym Sci 258:939
19. Möginger B (1993) Rheol Acta 32(4):370–379
20. Havránek A, Ilavský M, Nedbal J, Böhm M, Soden WV, Stoll B (1993) Rheol Acta 32:370
21. Eisenbach CD, Stadler E (1990) Colloid Polym Sci 268:636
22. Eisenbach CD, Steinlein C, Milius W (1994) Colloid Polym Sci 272:276
23. Matuszak ML, Frisch KC (1973) J Polym Sci Polym Chem Ed 11:637
24. Ferguson J, Petrovic Z (1973) Eur Polym J 12:117
25. Gassie N, Zulfiqar M (1978) J Polym Sci Polym Chem Ed 16:1563
26. Ballistreri S, Foti P, Maravigva G, Scamporrion E (1980) J Polym Sci Polym Chem Ed 18:1923
27. Petrovic S, Zavargo Z, Flynn JH, Mackinght WJ (1994) J Appl Polym Sci 51:1087
28. Lin MF, Tsen WC, Shu YC, Chuang FS (2001) J Appl Polym Sci 79:881
29. Rwei SP, Kao KC, Liou GS, Cheng KC, Guo W (2003) Colloid Polym Sci 281:407
30. Rwei SP, Liu AY, Liou GS, Cheng KC, Guo W (2004) Polym Eng Sci 44:376
31. Rwei SP, Cheng CY, Liou GS, Cheng KC (2005) Polym Eng Sci 45:478